Wind and Structures, Vol. 10, No. 3 (2007) 287-300
DOI: http://dx.doi.org/10.12989/was.2007.10.3.287

Wind velocity field during thunderstorms

Jacinto Ponte Jr.†

UNISINOS, Universidade do Vale do Rio dos Sinos, São Leopoldo, RS, Brasil

Jorge D. Riera‡

PROMEC/PPGEC, EE, Universidade Federal do Rio Grande do Sul, Porto Alegre, RS, Brasil
Av. Osvaldo Aranha 99, 3o. Andar, 90035-970, Porto Alegre, RS, Brazil

(Received November 24, 2005, Accepted May 4, 2007)

Abstract. Wind action is a factor of fundamental importance in the structural design of light or slender constructions. Codes for structural design usually assume that the incident mean wind velocity is parallel to the ground, which constitutes a valid simplification for frequent winds caused by meteorological phenomena such as Extratropical Storms (EPS) or Tropical Storms. Wind effects due to other phenomena, such as thunderstorms, and its combination with EPS winds in so-called squall lines, are simply neglected. In this paper a model that describes the three-dimensional wind velocity field originated from a downburst in a thunderstorm (TS) is proposed. The model is based on a semi empirical representation of an axially-symmetrical flow line pattern that describes a stationary field, modulated by a function that accounts for the evolution of the wind velocity with time. The model allows the generation of a spatially and temporally variable velocity field, which also includes a fluctuating component of the velocity. All parameters employed in the model are related to meteorological variables, which are susceptible of statistical assessment. A background wind is also considered, in order to account for the translational velocity of the thunderstorm, normally due to local wind conditions. When the translation of the TS is caused by an EPS, a squall line is produced, causing the highest wind velocities associated with TS events. The resulting vertical velocity profiles were also studied and compared with existing models, such as the profiles proposed by Vicroy, *et al*. (1992) and Wood and Kwok (1998). The present model predicts horizontal velocity profiles that depend on the distance to the storm center, effect not considered by previous models, although the various proposals are globally compatible. The model can be applied in any region of interest, once the relevant meteorological variables are known, to simulate the excitation due to TS winds in the design of transmission lines, long-span crossings, cable-stayed bridges, towers or similar structures

Keywords: thunderstorms, winds, downdraft, downburst, vertical profile, flutuaction, extreme value.

1. Introduction

Wind action is usually a factor of fundamental importance in structural design, especially in case of large spans and light structures. Codes for strucural design assume that in flat terrain the incident

† Professor of Industrial Engineering
‡ Professor of Civil Engineering, Corresponding Author, E-mail: JPONTE@unisinos.br

mean wind velocity vector is parallel to the ground, which constitutes a valid simplification for winds caused by the most frequent meteorological phenomena, such as Extratropical Storms, herein designated Extended Pressure Systems (EPS) or Tropical Storms (Hurricanes, Typhoons). On the other hand, wind effects due to other relevant meteorological phenomena, such as downbursts during thunderstorms (TS), and its combination with EPS winds in so-called squall lines, are simply neglected. In these events, the spatial distribution on any horizontal plane of the wind velocity maximum amplitude, as well as of its orientation, are far from uniform. Thus, TS wind fields differ significantly from models implicit in current codes, rendering the applicability of the latter to constructions with large dimension highly questionable. Moreover, TS wind records can hardly be regarded as samples of a stationary random process and their along wind fluctuating velocity components cannot be expected to be governed by surface roughness, as in case of EPS winds. Since the vertical velocity profiles are likewise different, both static and dynamic methods of analysis of tall, flexible structures subjected to wind action presently in use are not adequate to model the excitation due to TS events.

In temperate latitudes, in regions not affected by tropical cyclons, while roughly nine out of ten maximum annual velocity records at the standard 10m observation height occur during EPS events, extreme winds for design periods larger than about ten years are typically caused by TS events. In fact, Riera, *et al*. (1977) underlined a quarter of a century ago the need to assess the probability distribution of extreme *thunderstorm* wind velocities, sustained by the premise that the probability distribution of the maximum annual TS wind velocity at the reference 10 m height would be different from the distribution functions that describe the probability of occurrence of winds caused by extratropical (EPS) or by tropical storms. Thom (1968) had earlier proposed to deal with mixed populations of EPS and tropical storm winds by resorting to a combined probability distribution $P_V(v)$. At any rate, Riera and Nanni (1987) later confirmed, using data from 14 meteorological stations in southern Brazil that extreme annual EPS and TS winds are characterized by different probability distributions and that TS are the source of extreme winds in the low probability region. Recently the *IAWE Working Group WGF* proposed that *separate extreme value analysis for extreme winds from different storm types should be carried out when this is possible and known to be a feature of particular stations* (Holmes, *et al*. 2005). Models of TS events, as proposed herein, should be useful in implementing simulation analysis of rare events to complement or substitute meteorological records (Holmes, *et al*. 2005).

The frequency and magnitude of damage caused by thunderstorm, on the other hand, called the attention of engineers engaged in transmission line design and maintenance. In fact, more that 80% of failures of transmission line towers due to wind action in temperate climates occur during thunderstorms (CIGRÉ 2002). This evidence confirms the importance of TS winds in structural design, and justifies the growing interest in the phenomenon, which initiated, nevertheless, in aeronautical engineering. In this paper a model of the 3D wind field caused by a downdraft during a TS event is proposed, which accounts for the transient nature of thunderstorm winds as well as for its fluctuating components. The model may be applied in any region of interest, once the relevant meteorological variables are known, to simulate the excitation due to TS winds in the design of transmission lines, long-span crossings, cable-stayed bridges, tall towers and similar structures.

2. Description of the model: wind field in a stationary downburst

Thunderstorm winds are a consequence of the drowndraft that occurs when the ascending currents at the center of a mature cumulonimbus cloud reach altitudes above 10km, where the surrounding temperature, that may be as low as 50ºC below zero, rapidly cools the warm, humid air with a simultaneous increase in density. At this point, already in the region of the anvil, the heavier mix of cool air, water droplets and ice particles starts falling down by gravity, giving rise to the so-called *downburst* or *downdraft*. This accelerating column of air, water and ice, designated in meteorology as a *microburst* or a *macroburst* depending on its diameter, reaches, as it approaches the ground, axial velocities of the order of 30m/s. Downbursts caused several fatal aviation accidents. In fact, research on the topic started in Aeronautical Engineering in response to an obvious need to develop comprehensive models for the phenomenon (Fujita 1978).

Most models at this initial stage aimed at describing the flow field within a stationary mature cumulonimbus cloud. In addition to the assumption that the cloud does not move in relation to the ground, aspect of the problem that was of small relevance in aeronautical engineering, it was also considered that the flow regime was stationary, i.e., the velocity components varied with the spatial coordinates but not with time. A similar set of assumptions was adopted in wind tunnel studies of the phenomenon, in which a downburst was modelled by a stationary jet impinging on a flat surface (Wood and Kwok 1998). In this context, Riera and Rocha (1998) proposed an axi-symetric velocity field based on a solution developed by Zhu and Etkin (1985). The model constitutes a satisfactory approximation to the stationary flow and was adopted with some simplifications in the present formulation. Similar contributions were presented by Holmes and Oliver (2000) and Lecthford and Chen (2004).

Thus, in the following it is assumed that the causative cumulonimbus cloud is a circular cylinder with vertical axis. The base of the cylinder, i.e., of the cloud, is at height h above ground level. The flow lines are also assumed to be axisymmetrical in relation to the cloud vertical axis.

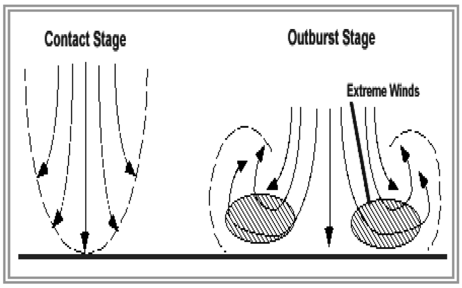

Fig. 1 Flow lines in TS (initial contact)

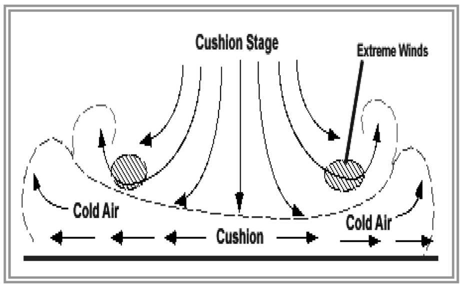

Fig. 2 Flow lines in TS (cushion stage)

Although the downdraft in a thunderstorm is a dynamic process in which temperature and air density change along the flow lines, it may be modelled with little error as an incompressible flow. According to McDonald and Fox (1995), the flow of gases with heat transfer can be considered incompressible when its Mach number $M = V/c_p$ is lower than 0.3, in which V denotes the flow velocity and c_p the velocity of sound. The Mach number in a downdraft is not expected to exceed about 0.20, so the flow should remain well within the range of validity of the hypothesis of incompressibility. Hence, applying Bernoulli's Theorem for heigths h and z above the ground, the tangential velocity at height z along a flow line is obtained:

$$V_t = [2 \int (dp/\rho)]^{1/2} \tag{1}$$

In which dp denotes a pressure differential while ρ is the specific mass. The dependence of the specifics mass on height was modeled by the following exponential function:

$$\rho(z) = \rho_o \exp(-\beta z) \tag{2}$$

The parameters in Eq. (2), estimated using data from McDonald and Fox (1995), are $\rho_o = 1{,}019$ kg/m^3 and $\beta = 0{,}0001$ are valid in the range $0 < z < 10000$ m. The pressure difference is assumed to vary linearly from zero at height h to ΔP_o at ground level. The pressure at height z can be written as:

$$p = \Delta P_o\,(1 - z/h) \tag{3}$$

introducing Eqs. (2) and (3) in Eq. (1) and solving the integral, the following expression for the tangential velocity is finally obtained:

$$V_t = [(2\,\Delta P_o) / (h\,\rho_o\,\beta)]^{1/2}\,[\exp(\beta h) - \exp(\beta z)]^{1/2} \tag{4}$$

Furthermore, available information indicates that the total pressure drop ΔP_o ranges between 100 and 500 Pa. but no statistical data was found to fit a probability density function to ΔP_o, which must then be modeled Solely on the basis of its estimated maximum and minimum values. For any given value of ΔP_o, Eq. (4) allows the determination of the tangential velocity. Typical velocity-height curves are shown in Fig. (3).

The axial and radial velocity components along a flow line can be determined once its equation is specified. Zhu and Etkin (1985) presented a simplified 3-dmensional model –the so called *doublet sheet model*- based in fluid mechanics considerations. For engineering purposes, the model was further simplified by Riera and Rocha (1998), to yield approximate expressions for the wind field during a TS event, maintaining the assumption of axial symmetry. In the following the flow lines are described by:

$$z(r) = k/r \tag{5}$$

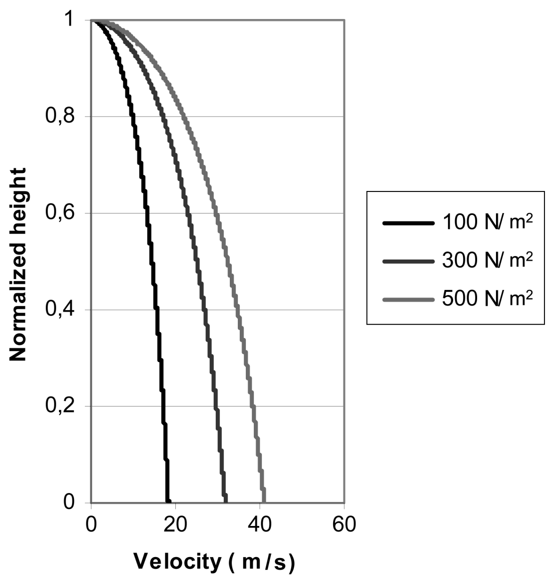

Fig. 3 Tangential velocity vs. height curves

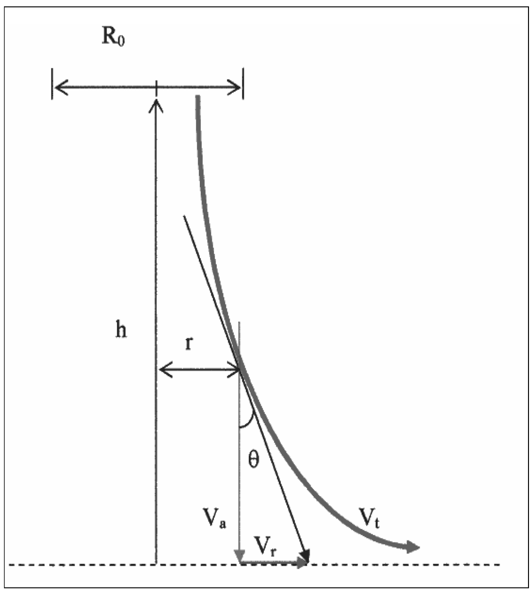

Fig. 4 Flow line in downdraft

k is a constant and r is the distance to the vertical axis of the cloud. The flow line assumed in expression (5) does not significantly differ from the models in the previous references or other proposals in the technical literature.

In fact, differences in predicted velocities are marginal. For a specific flow line, the derivative of z in relation the r, denoted $z'(r)$ defines the tangent of the angle in relation to Or axis. At point (r_p, h), the radial and axial velocity components for any height z of interest are given by:

$$V_r = V_t \{1/[1 + z'^2(r_p)]\}^{1/2} \tag{6}$$

$$V_a = V_t \{z'^2(r_p) / [1 + z'^2(r_p)]\}^{1/2} \tag{7}$$

$$r = [x^2 + y^2]^{1/2} \tag{8}$$

$$\sin \theta = \{1 / [1 + z'^2(r_p)]\}^{1/2} \tag{9}$$

$$\cos \theta = \{z'^2(r_p) / [1 + z'^2(r_p)]\}^{1/2} \tag{10}$$

in which θ denotes the angle between the tangent to the flow line and the vertical axis Oz. Finally, it results:

$$V_a = V_t [r_p^2 h^2/(r_p^2 h^2 + r^4)]^{1/2} \tag{11}$$

$$V_r = V_t [r^4/([r_p^2 h^2 + r^4)]^{1/2} \tag{12}$$

Denoting by R the distance from the axis of the downburst to a flow line, the axial and radial velocities are plotted in Figs. 5 and 6 for several flow lines, assuming a pressure drop ΔP_o = 200N/m^2 The velocity components in the direction of the coordinate axes are given by:

$$V_x = V_t \sin \theta \cos \beta = V_r \cos \beta \tag{13}$$

$$V_y = V_t \sin \theta \sin \beta = V_r \sin \beta \tag{14}$$

$$V_z = V_t \cos \theta = V_a \tag{15}$$

In which β denotes the angle between the projection of the flow line on a horizontal plane and the Ox axis.

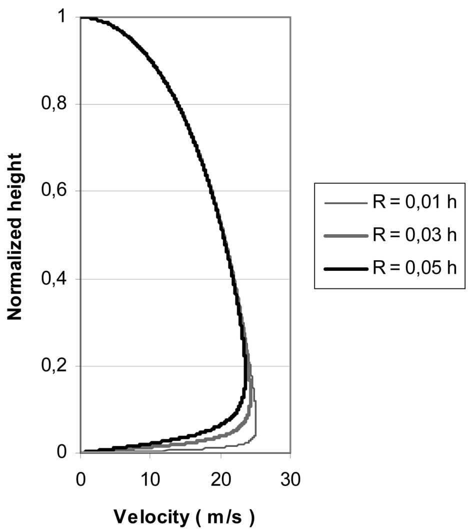

Fig. 5 Axial velocity vs. height curves

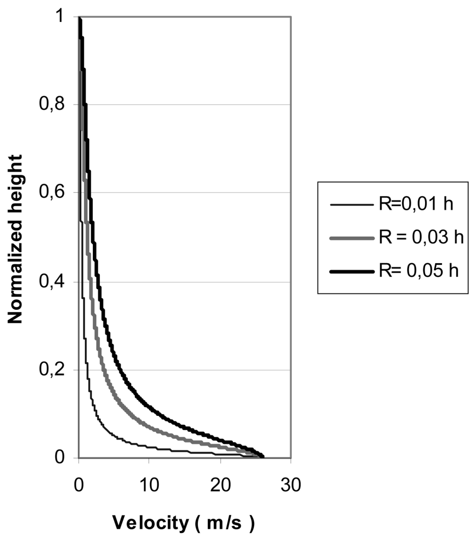

Fig. 6 Radial velocity vs. height curves

3. Translational velocity of the storm

The velocity field associated to a downdraft in a stationary cumulonimbus cloud was described in Section 2. The cumulonimbus cloud, whithin which the downdraft takes place, is usually carried along its path by a *background wind*. This wind may be caused by local atmospheric circulation, or due to an EPS event. Both are modeled in this paper by a horizontally stratified stationary flow, with constant mean velocity and orientation throughout the area of interest of about 400 km^2. It is assumed that the vertical velocity profile of the background wind is parabolic and depends on the surface roughness of the terrain in the upwind direction. It is also assumed that the resulting velocity vector at any point may be obtained as the vectorial sum of the stationary velocity vector, determined in Section 2, and the background wind velocity vector. If V_o denotes the modulus of the background wind velocity vector at a point, which forms an angle γ with the Ox axis, then the resultant velocity components in a reference cartesian coordinate system (xyz) are given by:

$$V_{Rx} = V_r \cos\beta + V_o \cos\gamma \tag{16}$$

$$V_{Ry} = V_r \sin\beta + V_o \sin\gamma \tag{17}$$

$$V_{Rz} = V_z \tag{18}$$

4. Evolution of the wind velocity with time

The wind velocity field described above assumes that the downdraft flow from the causative cloud is stationary. The resulting velocity amplitudes are thus upper bounds of the actual amplitudes, which vary with time defining a transient process. Following Holmes and Oliver (2000), the evolution of the wind velocity with time is herein represented by the equations:

$$V(t) = 1{,}58\ V_t\,[1-\exp(-t/T)],\ \text{for } t \le T \tag{19}$$

$$V(t) = V_t \exp\,[-(t-T)/T],\ \text{for } t > T \tag{20}$$

T denotes the storm *characteristic duration*, defined as the time at which the velocity attains its maximum value.

5. Horizontal velocity vertical profile

The *vertical profile of the horizontal component* of the wind velocity field at a given location has great interest in structural engineering, since it has a direct influence on the distribution of horizontal wind forces along the height of a construction at the location under consideration. The

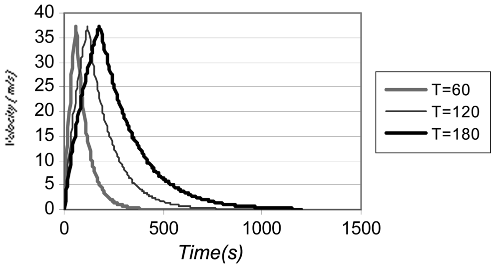

Fig. 7 Velocity-time functions in terms of T

model proposed herein predicts a vertical profile, for a stationary cloud, similar to the graph of radial velocities shown in Fig. 6. It may be seen that the profile depends on the position of the vertical axis of the cloud in relation to the location of interest. Also note that the velocity distribution illustrated by Fig. 6 does not take into account the roughness of the terrain, i.e. the existence of a boundary layer that would imply a decrease of the velocity as we approach the ground. Chen and Letchford (2004) recently presented a critical evaluation of models of the vertical profile for TS winds available in the literature. Oseguera and Bowles (1988) propose an empirical Eq. (21) for the average horizontal velocity caused by a downdraft:

$$V(z) = (\lambda R^2/2r)\{1-\exp[-(r/R)^2\}[\exp(-z/z_c)-\exp(-(z/z_d))] \tag{21}$$

In which λ denotes a scale factor with dimension $[T]^{-1}$, z_d a characteristic height (inside the boundary layer), z_c a characteristic height (outside the boundary layer), r the distance to the vertical axis of the downdraft cylinder and R the characteristic radius of the downdraft cylinder. Vicroy (1992), on the other hand, suggests the following equation for the velocity vertical profile:

$$V(z)= 1{,}22\ V_{\max}[\exp(-0{,}15\ z/z_m)-\exp(-3{,}2175\ z/z_m)] \tag{22}$$

In Eq. (22), $V_{\max}$ is the maximum velocity in the profile, while z_m denotes the height at which the maximum velocity occurs. A third model is due to Wood and Kwok (1998), who proposed the equation:

$$V(z) = 1{,}55\ V_{\max}(z/z_0)^{1/6}\ \{1-\Phi[0{,}7(z/z_0)]\} \tag{23}$$

In Eq. (23), z_0 represents the height where the speed is half the maximum value while Φ denotes the error function. Chen and Lechtford (2004) used the parameters indicated in Table 1 to build comparative profiles of the models listed above. More recentely Chay, *et al*. (2006) proposed a new Eq. (24) to define the vertical profile:

$$V(z) = (\lambda r/2)\ [\exp(c_1(z/z_m))-\exp(c_2(z/z_m))]\exp[(2-(r^2/r_p^2)^{\alpha})/2\alpha] \tag{24}$$

In which λ is a scale factor, α, c_1 and c_2 are constants, r is the radius r_p the radius at which the

Table 1 Parameters used to define the vertical profiles in Figs. 8 and 9

Parameters	Oseguera & Bowles	Vicroy	Chay, *et al.*	Wood & Kwok
r (m)	1121			
R (m)	1000			
z_d (m)	200			
z_c (m)	30			
λ (1/s)	0,414		0,595	
$V_{\max}$ (m/s)	80	80	80	80
$z_{\max}$ (m)	65	67	80	73
z_0 (m)				400
c_1			- 0,15	
c_2			-3,2174	
α			2	
r_p (m)			1500	

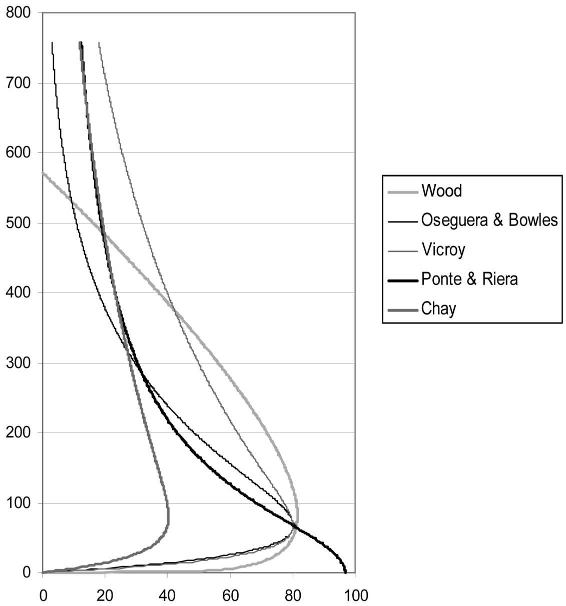

Fig. 8 Vertical profile at radius $r = 100$ m

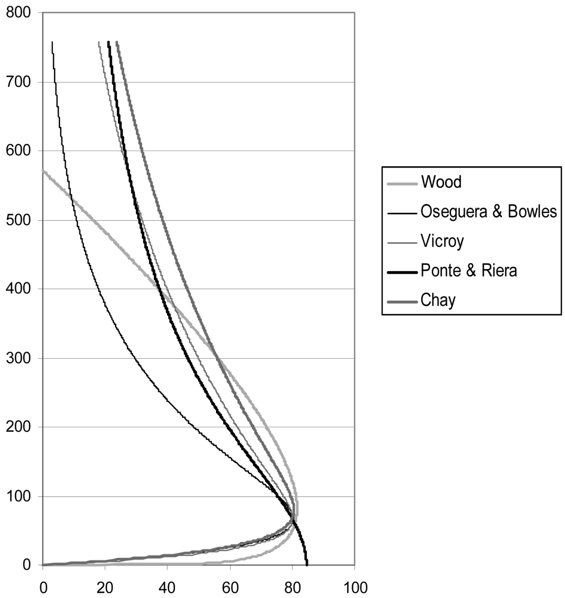

Fig. 9 Vertical profile at radius $r = 200$

maximum velocity occurs, z_m the elevation at which the maximum wind velocity occurs and z a generic elevation. Figs. 8 to 9 show the vertical profiles proposed in the literature, which are compared with profiles predicted by the model described in this paper. The graphs were normalized to present a common velocity of 80 m/s at a 67 m height above ground level. It may be seen that although the various models reflect specific features of EPS winds, such as the fact that the maximum velocity is attained at a height usually below 100 m and that the velocity steadily decreases for higher elevations, they present perceptible differences.

The present proposal approaches the model of Oseguera and Bowles (1998) when the distance to the cloud axis is around 100m. When the distance is about 200 m the model predictions approach Vicroy's (1992) equation. The model predictions are not close to Wood and Kwok (1998) results for any value of *r*. This poor correlation is attributed to the fact that Wood and Kwok (1998) equation is based on experimental observations in wind tunnel, and is therefore restricted to the experimental conditions, which do not faithfully reflect field conditions (Chen and Lecthford 2004).

The results presented above clearly illustrate the fact TS winds *are not characterized by a generic vertical velocity profile*, but by a family of profiles, depending on the distance from the location of interest to the path of the storm. In addition, since the causative cloud is typically in motion, the issue is further complicated by the fact that at least one additional factor should be considered, which is the ratio between the translational velocitiy of the cloud and the downdraft wind velocity.

6. Fluctuating velocity component

Under usual conditions, atmospheric flow in the lower boundary layer is turbulent. Turbulence manifests itself as fluctuations of the wind velocity around its average value. The magitude of the velocity vector in the direction of the flow may be written as:

$$V(t) = V_m(t) + \Delta V(t) \tag{25}$$

In which $V(t)$ denotes the instantaneous velocity at time t, $V_m(t)$ the mean velocity and $\Delta V(t)$ the fluctuating longitudinal velocity component. When the flow is stationary, the mean velocity V_m does not depend on time. In such case, Eq. (25) can alternatively be written in the form: (Davenport 1961):

$$V(t) = V_o[1 + I\phi(t)] \tag{26}$$

In which V_o is a mean reference velocity, I the intensity of turbulence and $\phi(t)$ a stationary random process with zero mean and unitary standard deviation. The intensity of turbulence is defined as the quotient between the standard deviation of the longitudinal velocity fluctuations and the mean velocity (Simiu and Scanlan 1992, Blessmann 1995). The random process $\phi(t)$ is defined by its power spectral density function (psdf), for which a number of models have been proposed in the technical literature, such as those due to Davenport, Von Karman, Kaimal and Harris (Simiu and Scanlan 1992, Blessmann 1995). However, all these spectral density functions are only applicable when vertical stability of the atmosphere prevails and the turbulence in the lower boundary layer results mainly from the interaction of the flow with the rough surface. Note that a minimum stretch is needed to develop a given profile and turbulence intensity,. The length of this so-called *exposure terrain* is of the order of one kilometer or more, condition that is not satisfied by TS winds, in which the flow lines remain close and approximately parallel to the ground for a few hundred meters. Thus, there seems to be no reason to expect that the psdf of the velocity fluctuations in TS winds will be satisfactorily modelled by the functions normally employed for EPS winds.

A purely empirical approach to the problem seems of little use, on account of the large number of factors discussed in connection with the vertical profile, which should also influence the turbulence spectra. However, a preliminary analysis of TS wind records revealed peaks in the psdf´s of the fluctuations, in the frequency band between 0,05 and 0,55Hz, with no prevailing frequency. A very simple model for the longitudinal turbulence in TS events was then parsimoniously adopted: a band-pass white noise, with frequency limits as quoted above. In order to simulate such process in preliminary applications, the velocity fluctuations were expressed as $V_o\, I\, \phi\,(t)$, with:

$$\phi\,(t) = A_1(t)\sin(\omega_m\, t) + A_2(t)\cos(\omega_m\, t) \tag{27}$$

$$A_1(t) = \sin(\omega_L\, t) \tag{28}$$

$$A_1(t) = \cos(\omega_L\, t) \tag{29}$$

In which A_1 and A_2 are functions of the lower cut-off frequency ω_L, while ω_m denotes the median frequency between ω_L and the upper cut-off frequency ω_u, that depends on the power spectral density function to be simulated (Lathi 1968). Introducing Eqs. (28) and (29) into Eq. (27) leads to the equivalent generic equation

$$\phi(t) = a\cos[(\omega_m - \omega_L)t + \theta] \tag{30}$$

in which θ is a random phase angle caracterized by a uniform probability distribution function within the $[0, 2\pi]$ interval. Fig. 10 shows a sample of the velocitiy-time function for a TS event with characteristic duration T = 60s, maximum tangential velocity equal to one and intensity of turbulence I = 0, 50. The vertical and horizontal axis represent the velocity in (m/s) an the time in (s) respectively.

Horizontal wind velocity vs. time records at various heights measured in a 40m tall observation tower by Paluch, *et al.* (2003) are shown in Fig. 11. It may be seen that the velocity of the background wind, around 10m/s, slightly increases with height. However the transient due to a typical TS event that reached the station at about 2:12 PM, is characterized by a nearly constant vertical profile up to the tower height. In addition, the fluctuating components during the about 12min long TS event are almost perfectly correlated along the tower height. The similarity between recorded and simulated velocity records is apparent. Unfortunately, no additional information was in this case available to determine the distance between the observation tower and the storm path.

7. Practical applications

As underlined in the introductory comments, an important area of application of the model of a TS wind field presented in this paper is risk assessment through simulation analyses. An illustrative

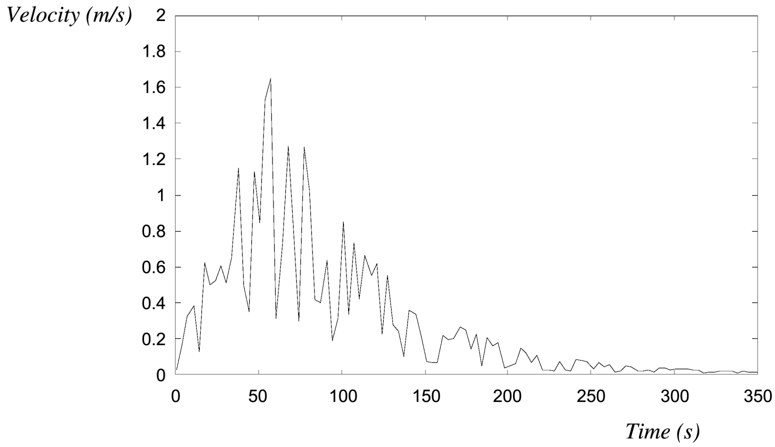

Fig. 10 Velocity-time plot for sample TS event

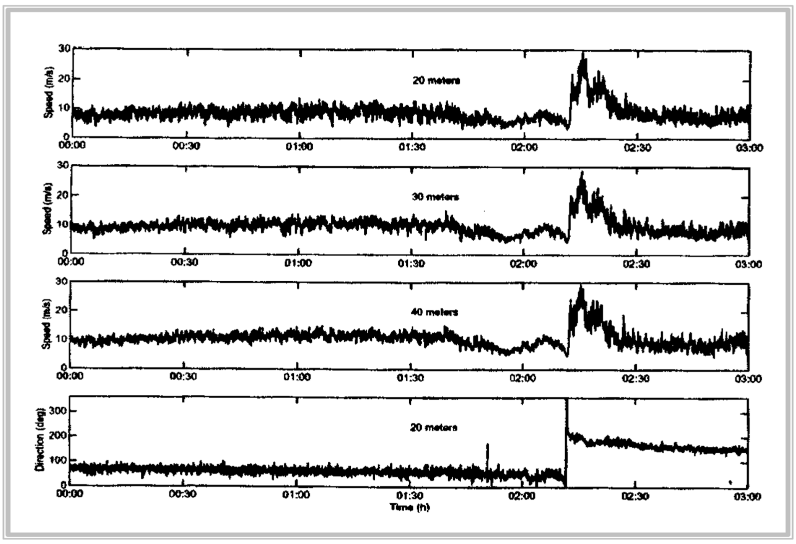

Fig. 11 Velocity-time record during a TS event at 20, 30 and 40m height (from Paluch, *et al.* 2003)

example is described in this section, which consists of the determination of a *worst case* TS wind excitation on one of the towers of São José do Norte crossing. The probabilistic characterization, for areas of interest in Brazil, of the parameters used in the model is currently in progress. It should be expected that some of these parameters will present non-negligible cross-correlations, issue that appears to be particularly relevant for risk studies. Thus, for purposes of illustration, parameters that present approximately 20% probability of being exceeded were adopted, leading to a nominal *worst case* storm. Note that very scarce statistical data is available on the physical variables that characterize TS events, such as pressure drop or the cloud dimensions, subject that is presently under study.

The crossing is part of a 69 KV transmission line that extends from São José do Norte to Rio Grande, in southern Brazil (Paluch, *et al*. 2005). Fig. 12 indicates the tower dimensions and other features of the structure.The surface roughness of the area around the crossing ranges, depending on the incident wind orientation, from Terrain Categories 1 to 3, according to the Brazilian Wind Code NBR 6123 (1983). The left support of the central span consists of a concrete tower, 120 m tall, that in turn supports a steel truss 10.95 m tall, as shown in Fig. 12.

In accordance with the worst case situation described before, it was assumed that the path of the TS exactly crosses the centerline of the tower. The wind velocity was computed at four elevations, namely $h = 30$, 60, 90 and 120 m, that is, at 30 m intervals, for two values of the translational velocity at a 10 m reference height $V_0 = 10$ m/s and 30 m/s. A characteristic duration equal to $T =$ 60s, and a pressure drop $\Delta P_o = 300$ N/m^2 were assumed, while the distance from ground level to the center of the anvil was adopted as 10 km. Two initial locations of the storm (x_o, y_o) were simulated, at distances of 600 m and 1800 m of the tower. Turbulence was disregarded, to allow a clearer perception of the difference with the design velocity distribution according to the current brazilian code NBR6123. Moreover, the variation of the translational velocity with height is defined by:

$$V(z) = V_0\,(z/10)^{p} \tag{31}$$

In which the exponent $p = 0.16$, corresponding to open terrain with few obstacles, was adopted

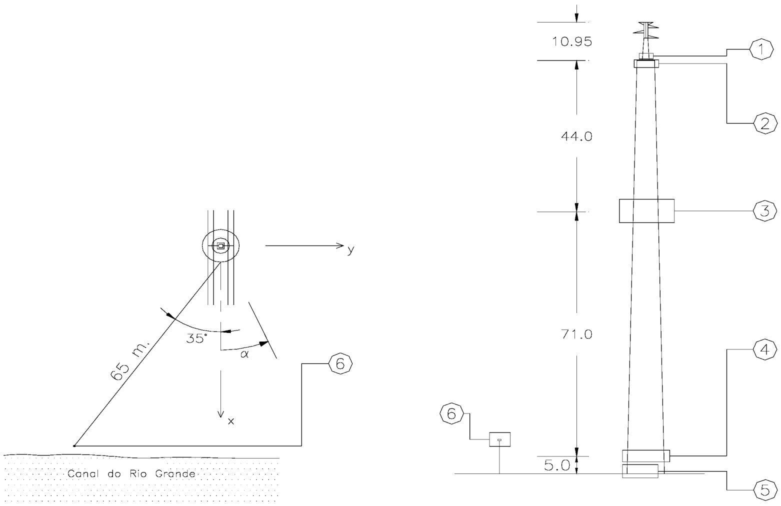

Fig. 12 Concrete tower and lattice steel tower on top

(x_o, y_o) = (0, -1800 m) and V_0 = 30 m/s

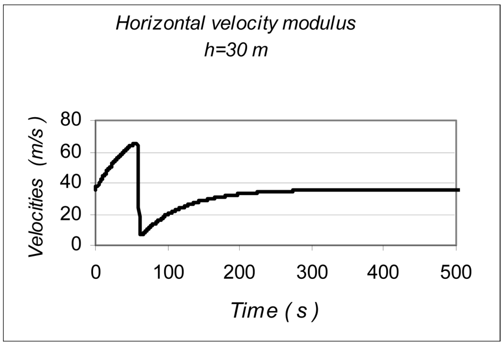

Fig. 13 Modulus of horizontal velocity V_h

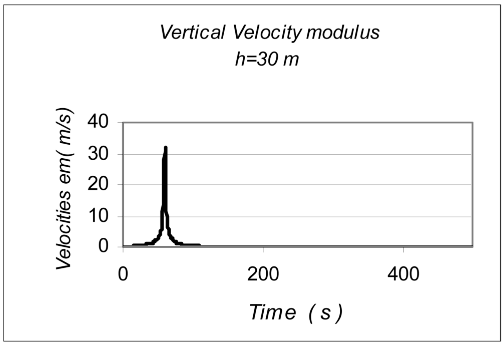

Fig. 14 Modulus of vertical velocity Vz

The evolution of the horizontal velocity modulus and the modulus of the vertical velocity at a 30m height are shown in Figs. 13 and 14. At other heights, the shapes of the velocity-time functions are quite similar, changing only in amplitude. Additional data is presented in Tables 3 and 4. The coordinates of the center of storm and the translational velocity are (x_o, y_o) = (0,01 m, -1800 m) and V_o = 30 m/s in the first axample and (x_o, y_o) = (0,01 m, -600 m) and V_o = 10 m/s in the second example. These velocities would correspond to typical EPS winds, in a squall line, and to a general circulation background wind, respectively.

Table 4 also includes design velocities for a 50 years mean recorrence period, at the various heights, according to the current code NBR 6123, which is based on the implicit assumption that wind is caused by EPS events. These velocities are largely exceeded by the simulated squall line storm in the adjacent column, although no probability of occurrence has yet been established for the later.

Table 3 Peak velocities for ΔP_o = 300 N/m^2 and V_o = 10 m/s at position (0, -600 m)

Height	Horizontal velocity (TS+Background Wind)	Vertical velocity (TS+Background Wind)
30 m	39,2 m/s	30,4 m/s
60 m	40,1 m/s	30,9 m/s
90 m	40,0 m/s	32,9 m/s
120 m	39,4 m/s	33,7 m/s

Table 4 Peak velocities for ΔP_o = 300 N/m^2 and V_o = 30 m/s at position (0, -1800 m)

Height	Horizontal velocity - NBR 6123	Horizontal velocity (TS+EPS)	Vertical velocity (TS+EPS)
30 m	47,5 m/s	65,3 m/s	25,4 m/s
60 m	51,1 m/s	71,2 m/s	34,2 m/s
90 m	53,3 m/s	73,3 m/s	35,5 m/s
120 m	54,9 m/s	74,5 m/s	35,7 m/s

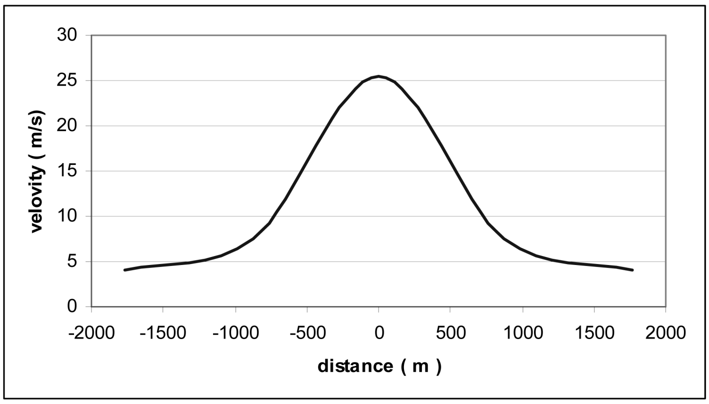

Fig. 15 Evolution of vertical velocity with distance to storm vertical axis (x_o= 0, y_o= -600 m and V_o = 10 m/s)

The vertical velocity component, indicated in last column of Table 4, may be important for the design of special structures, such as light roofs, when the axis of the storm crosses the control point. This effect can be seen in Fig. 15 which shows the evolution of the maximum vertical component at 10m height with the distance to the storm vertical axis. The curve may be viewed as an upper limit of the vertical velocity component in terms of the horizontal distance between the location of interest and the storm path.

8. Conclusions

A robust model for the wind velocity field during thunderstorms was proposed in the paper, taking into consideration all features of the phenomenon considered relevant for the design of structures subjected to wind action. The model predictions are compatible with available evidence concerning, for example, storm duration or vertical velocity profiles. Moreover, the formulation of the model requires a number of parameters that have ranges of variation reasonably well defined in Meteorology, allowing risk assessments even in situations in which scarce data is available for the region of interest.

Acknowledgements

The writers wish to acknowledge the partial support of CNPq and CAPES (Brazil). The writers also acknowledge the valuable remarks of the Reviewers, which led to significant improvements of the paper.

References

ABNT- Associação Brasileira de Normas Técnicas. (1987), "*Ação do Vento nas Edificações*", Norma NBR-6123, Rio de Janeiro, 1987.

Blessmann, J. (1995), *O Vento na Engenharia Estrutural*, Editora da Universidade, 1ª edição, Porto Alegre, RS, Brasil..

Caracena, F., Holle, R. L. and Dosswe llIII, C. A. (1977), *Microbursts: A handbook for visual identification.* NOAA, National Severe Storm Laboratories, U.S.A., December 1977.

CIGRÉ SC22 WG16- (2002), Meteorology for overhead lines- *Draft Report on Current Practices regarding*

Frequencies and Magnitude of High Intensity Winds- Aug. 2002.
Chay, M. T., Albermani, F. and Wilson, B. (2006), "Numerical and analytical simulation of downburst wind loads", *Eng. Struct*, **28**, 240-254.
Chen, Ching L. and Lectchford, C. W. (2004), "A deterministic-stochastic hybrid model of downburst and its impact on a Cantilivered Structure", *Eng. Struct*, **26**, 619-626.
Fujita, T. T. (1978), Manual of downburst identification for Project NIMROD, SMPR-156. University of Chicago, may 1978.
Fujita, T. T. (1985), *The Downburst Microburst and Macroburst* – Report of projects NIMROD and JAWS. 1985.
Holmes, J. D. and Oliver, S. E. (2000), "An empirical model of a downburst", *Eng. Struct,* Elsevier, **22**, 1167-1172.
Holmes, J. D., Baker, C. J., English, E. C. and Choi, E. C. C. (2005), "Wind structures and codification", *Wind Struct*, **8**(4), 235-250.
Holmes, J. D, Kasperski, M., Miller, C. A., Zuranski, J. A. and Choi, E. C. C., "Extreme wind prediction and zoning", *Wind Struct*, **8**(4), 269-281.
Lathi, B. P. (1988), *Sistemas de comunicação*, Editora Guanabara , Rio de Janeiro, Brasil.
McDonald, Alan T. and Fox, Robert W. (1995). "*Introdução à Mecanica dos Fluidos*", Editora Guanabara Koogan S.A. 4a. Edição. Copyritght 1995.
Oseguera, R. M. and Bowles, R. L. (1988), "A Simple Analytic 3-Dimensional Downburst Model Based on Boundary Layer Stagnation Flow", *NASA Technical Memorandum 100632*, July 1988.
Paluch, M. J., Toazza, A., Rocha, M. M. and Marroquim, A. I. (2003), "O laboratório anemométrico da Universidade de Passo Fundo", *III Workshop Brasileiro de Micrometeorologia*; UFSM, Universidade Federal de Santa Maria, Santa Maria, RS, Brasil, 201-205, 2003.
Paluch, M. J., Cappellari, T. T. O. and Riera, J. D. (2007), "Experimental and numerical assessment of EPS wind action on long span transmission line conductors", *J. Wind Eng. Ind. Aerodyn,* Elsevier, The Netherlands, (to be published).
Ponte Jr, Jacinto (2006), "Modelagem e Simulação do Campo de Velocidades do Vento em Tormentas Elétricas", *Tese de Doutorado.* Promec, UFRGS., Porto Alegre, RS, Brasil, 2005.
Riera, J. D., Viollaz, A. J. and Reimundin, J. C. (1977), "Some recent results on probabilistic models of extreme wind speeds", *J. Industrial Aerodyn,* Elsevier, The Netherlands, **2**, 271-287.
Riera, J. D. and Nanni, L. F. (1989), "Pilot study of extreme wind velocities in a mixed climate considering wind orientation", *J. Wind Eng. Ind. Aerodyn,* Elsevier, The Netherlands, Vol. **32**, 11-20.
Riera, J. D. and Rocha, M. M. (1998), "Load definition for wind design and reliability assessments; extreme wind climate", *Wind Effects on Buildings and Structures*, (J. D. Riera & A. G. Davenport, Editors), A. A. Balkema, Rotterdam, 1998.
Simiu, E. and Scanlan, R. H. (1996), *Wind Effects on Buildings and Structures,* Third Edition, John Wiley & Sons, Inc., New York, USA, 1996.
Thom, H. C. S. (1967), "Toward a universal climatological extreme wind distribution", *Wind Effects on Buildings and Structures,* Ottawa, Canada, Univ. of Toronto Press, **1**, 669-684.
Vicroy, D. D. (1991), "A simple, analytical,axisymmetric microburst model for downdraft estimation", *NASA TM-104053*, DOT/FAA/RD, 91/10, Feb-1991.
Vicroy, D. D. (1992), "Assessment of microburst models for downdraft estimation", *J. Air Craft*, **29**, 1043-1048.
Wood, G. S., and Kwok, C. S. (1998), "An empirically derived estimate for the mean velocity profile of a thunderstorm downburst", *7 th AWES Workshop*, Auckland, Australia, 1998.
Zhu, S. and Etkin, B. (1985), "Model of the wind field in a downburst", *J. Aircraft*., **22**(7), 595-601, July 1985.

Sites references

WW 2010 on line Gides. University of Illinois .
http://ww2010.atmos.uiuc.edu/(Gh)/guides/mtr/svr/comp/out/micro/home.rxml

CC